Eucommia ulmoides extract attenuates angiotensin II-induced cardiac microvascular endothelial cell dysfunction by inactivating *p53*

Liye Hu[1], Xiaolin Xu[2], Xunli Xiao[1*]

[1]Department of Pharmacy, Affiliated Hospital of Jinggangshan University, Ji'an, P.R. China,
[2]Department of Pharmacy, Ji'an Hospital of Shanghai East Hospital, Ji'an, P.R. China

Angiotensin II (AngII) causes endothelial dysfunction. *Eucommia ulmoides* extract (EUE) is documented to manipulate AngII, but its impact on cardiac microvascular endothelial cell (CMVEC) function remains unknown. This study determines the effects of EUE on AngII-treated CMVECs. CMVECs were treated with different concentrations of AngII or EUE alone and/or the p53 protein activator, WR-1065, before AngII treatment, followed by examinations of the apoptotic, migratory, proliferative, and angiogenic capacities and nitric oxide (*NO*), *p53*, von Willebrand factor (*vWF*), endothelin (*ET*)-*1*, endothelial NO synthase (*eNOS*), manganese superoxide dismutase (*MnSOD*), hypoxia-inducible factor (*HIF*)-*1α*, and vascular endothelial growth factor (*VEGF*) levels. AngII induced CMVEC dysfunction in a concentration-dependent manner. EUE enhanced the proliferative, migratory, and angiogenic capacities and *NO*, *MnSOD*, and *eNOS* levels but repressed apoptosis and *vWF* and *ET-1* levels in AngII-induced dysfunctional CMVECs. Moreover, AngII increased *p53* mRNA levels, p-p53 levels in the nucleus, and p53 protein levels in the cytoplasm and diminishes *HIF-1α* and *VEGF* levels in CMVECs; however, these effects were counteracted by EUE treatment. Moreover, WR-1065 abrogated the mitigating effects of EUE on AngII-induced CMVEC dysfunction by activating *p53* and decreasing *HIF-1α* and *VEGF* expression. In conclusion, EUE attenuates AngII-induced CMVEC dysfunction by upregulating *HIF-1α* and *VEGF* levels via *p53* inactivation.

Keywords: Eucommia ulmoides extract. Angiotensin II, Cardiac microvascular endothelial cell, p53 activation, Dysfunction

INTRODUCTION

Endothelial cells account for one-third of all cardiac cells and perform vital functions in the maintenance and support of coronary microvasculature and neighbouring cardiomyocytes under normal conditions as well as angiogenesis under pathophysiological conditions (Liao *et al.*, 2021). Cardiac microvascular endothelial cells (CMVECs) originate from coronary vessels and serve crucial functions in angiogenesis induction and oxygen and nutrient delivery to the myocardium (Fan *et al.*, 2019). Dysfunctional endothelial cells are distinguished by aberrant extracellular matrix and decreased viability and migration, eventually leading to the development of pathological conditions (Kim, Piao, Hong, 2021). CMVEC dysfunction is associated with numerous conditions, such as radiation-induced heart disease, myocardial ischaemia, and heart failure related to type 2 diabetes (Li *et al.*, 2021; Zeng *et al.*, 2020). Hence, it is of considerable interest to study CMVEC dysfunction to develop effective treatment methods for cardiac diseases.

Angiotensin II (AngII) is a biologically active peptide that modulates vessel tone, facilitates the proliferation of vascular smooth muscle cells, and assumes crucial roles in the aetiology of cardiovascular conditions (Li *et al.*, 2015). Excess AngII in the circulation and tissues results in a pro-hypertrophic, pro-fibrotic, and pro-inflammatory environment, leading to dysfunction and remodelling

***Correspondence:** X. Xiao. Department of Pharmacy. Affiliated Hospital of Jinggangshan University. No. 110, Jinggangshan Ave, Jizhou District, Ji'an, Jiangxi 343000, P.R. China. E-mail: xiaoxunli197308@163.com. ORCID: https://orcid.org/0000-0002-6402-2220

of renal and cardiovascular tissues (Ames *et al.*, 2019). AngII induces CMVEC apoptosis in a dose-dependent manner (Wang *et al.*, 2019). Therefore, AngII may act on cardiovascular diseases by inducing CMVEC dysfunction.

Eucommia ulmoides (E. ulmoides) is a Chinese herbal medicine that has been used for its anti-hypertensive, diuretic, immunomodulatory, anti-bacterial, anti-aging, anti-inflammatory, anti-neoplastic, analgesic, antioxidant, hypoglycaemic, and hypolipidaemic effects since the past 2000 years (Lee *et al.*, 2005; Liu *et al.*, 2012; Park *et al.*, 2006; Wang *et al.*, 2016). To date, 205 ingredients, including phenols, polysaccharides, lignans, flavonoids, terpenoids, steroids, and iridoid terpenoids, have been identified in *E. ulmoides* (Liu *et al.*, 2020). *E. ulmoides* is used to treat various conditions, such as hypertension, osteoporosis, rheumatoid arthritis, impotency, forgetfulness, seminal emission, and menopausal syndrome in Chinese medicine and has gained attention for its therapeutic effects against hyperglycaemia, hypertension, osteoporosis, diabetes, obesity, sexual dysfunction, aging, and Alzheimer's disease in modern pharmacological research (He *et al.*, 2014). Lignans, major bioactive constituents of *E. ulmoides*, could prevent endothelial dysfunction by modulating the nuclear factor E2-related factor 2/ heme oxygenase-1 pathway and can be used to treat microvascular dysfunction caused by diabetes (Liu *et al.*, 2016). Lignans (300 mg/kg) treatment elevates plasma nitric oxide (NO) levels and decreases AngII levels in rats with spontaneous hypertension (Luo *et al.*, 2010).

p53, a transcription factor, is involved in various processes, such as cell cycle distribution, apoptosis, intracellular signalling, DNA repair, metabolism, and modulation of cellular interactions (Naryzhny, Legina, 2019). Suppression of *p53* reduces apoptosis and enhances tube-forming ability of coronary endothelial cells (Si *et al.*, 2020). AngII upregulates *p53* expression and activates the *p53* pathway in hypertensive kidney cells (Long *et al.*, 2021). AngII also induces dynamin-related protein 1 expression by promoting p53 acetylation, resulting in cardiomyocyte apoptosis (Qi *et al.*, 2018). Hypoxia-

inducible factor (*HIF*)-*1α* expression is mainly localised in the nucleus and decreased by *p53* activation in ovarian cancer cells (Zhang *et al.*, 2019). Moreover, activation of *HIF-1α* induces the transcription of vascular endothelial growth factor (*VEGF*), facilitating angiogenesis (Rana, Singh, Koch, 2019). Based on these reports, we hypothesized that *E. ulmoides* extract (EUE) interacts with *p53* to regulate *HIF-1α* and *VEGF* expression, thereby influencing the impact of AngII on CMVECs. To verify this, we explored the effects of EUE and *p53* on AngII-treated CMVECs in this study.

MATERIAL AND METHODS

Cell culture

Human CMVECs (CP-H079; Procell, Wuhan, China) were cultured in Dulbecco's modified Eagle's medium (Gibco, Grand Island, NY, USA) with 10% foetal bovine serum (Thermo Fisher Scientific, Wilmington, DE, USA) and antibiotics (Gibco) at 37 °C with 5% CO_2. Cell morphology was observed daily and the medium was renewed.

Construction and treatment of an endothelial cell dysfunction model

An endothelial cell dysfunction model was constructed as previously described (Li *et al.*, 2020). Briefly, CMVECs were incubated at 37 °C for 48 h in a medium containing different concentrations of AngII (10^{-8}, 10^{-7}, 10^{-6}, and 10^{-5} M) (experimental group) or an equal amount of normal saline (control group) with 5% CO_2.

To determine the effects of EUE on CMVECs, CMVECs in the experimental group were subjected to 1-h treatment with media containing variable concentrations of EUE (0.25, 0.5, 1, and 2 mg/mL; Naturalin, Changsha, China), followed by AngII (10^{-5} M) treatment. To further determine the effects of p53 on CMVECs, CMVECs in the experimental group were subjected to 1-h of combined treatment with EUE (1 mg/mL) and the p53 protein activator, WR-1065 (100 µmol/L; Sigma-Aldrich, St Louis, MO, USA) before AngII (100 nmol/L)

treatment. Cells in the control group were treated with equal amounts of normal saline.

3-(4, 5-dimethylthiazol-2-yl)-2, 5-diphenyltetrazolium bromide (MTT) assay

CMVECs were seeded in a 96-well plate (5×10^3 cells/well) and treated for 2 h with MTT solution (10 μL/well; M6494; Thermo Fisher Scientific). Each sample was set up in three replicates. Reaction was terminated with dimethyl sulfoxide (Sigma-Aldrich), with the absorbance assessed at 490 nm using a microplate reader (Model 680; Bio-Rad, Hercules, CA, USA).

Scratch assay

Scratch assay was conducted as previously described (Cao *et al.*, 2022). After seeding in a 6-well plate (5×10^5 cells/well) and reaching 80% confluency, CMVECs were scratched with a pipette tip, eluted once with the serum-free medium, and observed and photographed under a low-power phase-contrast microscope (Olympus, Tokyo, Japan) for comparison and statistical analyses. CMVECs were incubated for 48 h in a serum-free medium at 37 °C in a 5% CO_2 incubator and photographed again for recording. Image Pro Plus software was employed to measure the migratory capacity of cells.

Tube formation assay

Matrigel (Corning, Tewksbury, MA, USA) was dissolved in a 48-well plate (Millipore, Billerica, MA, USA) at 4 °C, and pipette tips were pre-cooled. Matrigel (100 μL) was added to the 48-well plate, gently shaken, mixed, and solidified in incubators for 30 min. Each well was subjected for 5-h incubation with CMVECs (2×10^4 cells/well) at 37 °C and 5% CO_2, with three replicates. Three fields of view were randomly selected to count the number of tubular structures.

Flow cytometry

Flow cytometry was employed to determine the expression of the CMVEC surface marker, CD31. After reaching 80% confluency, CMVECs were washed twice with phosphate-buffered saline (PBS) and reacted with 4 mL of digestion solution (0.25% trypsin and 0.01% ethylene diamine tetraacetic acid) for 30 s, followed by supplementation with an equal volume of complete medium to stop the reaction. After gentle trituration, cells were completely detached and triturated to form a single-cell suspension. Cell suspension was centrifuged at 1000 rpm for 5 min, and cell precipitate was resuspended in l mL PBS and blocked with 10% normal goat serum to prevent non-specific binding. In each Eppendorf tube, 100 μL of the cell suspension was cultured with 5 μL fluorescein isothiocyanate (FITC)-labelled anti-CD31 (1 μg/mL; ab9498; Abcam, Cambridge, UK) at 4 °C for 30 min in the dark. Antigen expression was determined using a flow cytometer (CytoFLEX; Beckman Coulter, Brea, CA, USA), and the results were analysed using the FlowJo software (Tree Star, Ashland, OR, USA).

Cell apoptotic capacity was determined using the Annexin V-FITC Apoptosis Detection Kit (Beyotime, Shanghai, China). Cells were trypsinised, centrifuged, resuspended in a binding buffer, and cell concentration was adjusted to 1×10^6 cells/mL. Cells were then incubated with 5 μL Annexin V-FITC and propidium iodide for 15 min in the dark at room temperature, followed by evaluation of apoptosis levels using a flow cytometer.

Measurement of NO levels

NO levels in the cell supernatant were measured using an NO assay kit (Nanjing JianCheng Bioengineering Institute, Nanjing, China), as previously described (Li *et al.*, 2020). Briefly, samples were mixed and incubated with reagents 1 and 2 at 37 °C for 60 min, supplemented with reagents 3 and 4, mixed for 30 s, incubated for 40 min at room temperature, and centrifuged at 3500 rpm for 10 min. Then, the supernatant (0.5 mL) was harvested, added to a colour developer, and incubated for 10 min at room temperature. Absorbance at 550 nm was determined using a microplate reader (Model 680; Bio-Rad), and NO levels were calculated.

Reverse transcription-quantitative polymerase chain reaction (RT-qPCR)

Total cellular RNA was extracted using the Trizol reagent, and RNA purity and concentration were determined using a NanoDrop micronucleic acid analyzer. RNA was reverse transcribed into cDNA using the PrimeScript RT kit (RR036A; Takara, Kyoto, Japan) with a 10 μL reverse transcription system. Reaction conditions were set as follows: reverse transcription at 37 °C for 15 min (3 times) and reverse transcriptase inactivation at 85 °C for 5 s. Reaction solution was analysed via fluorescent qPCR using the TB Green Premix Ex Taq II kit (RR820A; Takara) with a 50 μL reaction system [25 μL SYBR Premix Ex TaqTM II (2 ×), 2 μL PCR upstream primers, 2 μL PCR downstream primers, 1 μL ROX Reference Dye (50 ×), 4 μL DNA template, and 16 μL ddH2O] on an ABI7500 quantitative PCR instrument (7500; Applied Biosystems, Foster City, CA, USA). Reaction conditions were as follows: pre-denaturation at 95 °C for 30 s, 40 cycles of denaturation at 95 °C for 5 s, and annealing and extension at 60 °C for 30 s. Relative levels of the genes were determined using the $2^{-\Delta\Delta CT}$ method with 2 μg of total RNA as the template and glyceraldehyde-3-phosphate dehydrogenase (*GAPDH*) as the internal reference. All primer sequences used in this study are listed in Table I.

TABLE I - Primer sequences

Gene	Sequence (5'-3')
p53-F	TCCCAAGCAATGGATGATTT
p53-R	GTCACAGACTTGGCTGTCCC
Hif-1α-F	AGAGGTTGAGGGACGGAGAT
Hif-1α-R	CTCCGACATTGGGAGCTCAT
VEGF-F	TCACCAAGGCCAGCACATAG
VEGF-R	GAGGCTCCAGGGCATTAGAC
GAPGH-F	GGTGAAGGTCGGAGTCAACG
GAPDH-R	TGAAGGGGTCATTGATGGCAAC

Note: F, forward; R, reverse.

Western blotting

Nuclear and cytoplasmic proteins were extracted using the nuclear/cytoplasmic protein isolation kit (BioVision, Mountain View, CA, USA), and protein concentrations were assessed using a bicinchoninic acid assay kit (Beyotime). First, proteins were denatured with a loading buffer in a boiling water bath for 10 min, and the sampling volume was calculated based on the protein loading volume. After loading, proteins were electrophoresed at 80 V for 30 min and then at 120 V for 90 min after bromophenol blue entered the separation gel and transferred to membranes at a current of 250 mA in an ice bath for 100 min. Then, the membranes were washed thrice with the washing solution for 1–2 min each time, blocked for 2 h in a blocking solution, and probed with primary antibodies (1:1000; Abcam) against p53 (ab26), phosphorylated p53 (p-p53; ab33889), von Willebrand factor (vWF; ab6994), endothelin-1 (ET-1; ab2786), endothelial NO synthase (eNOS; ab199956), manganese superoxide dismutase (MnSOD; ab68155), HIF-1α (ab179483), and GAPDH (ab8245) and primary antibodies against VEGF (1:1000; AF5131; Affinity Biosciences, Jiangsu, China) overnight at 4 °C. Membranes were washed thrice for 10 min each with Tris-buffered saline with Tween 20 (TBST), re-probed for 2 h with secondary Immunoglobulin G antibodies at room temperature, and washed thrice for 10 min with TBST. Then, the membranes were developed with an electrogenerated chemiluminescence solution (P0018FS; Beyotime) and examined using a chemiluminescent imaging system (Bio-Rad). Relative expression levels of proteins were calculated as the ratio of the gray value of the target band to that of the internal reference band, with GAPDH as the internal reference.

Statistical analysis

Data were statistically analysed using GraphPad Prism 7 software and summarized as the mean ± standard deviation. Comparisons between two groups were analysed using the *t*-test, and comparisons among multiple groups were analysed using one-way analysis of variance with post-hoc multiple comparisons using Tukey's multiple comparisons test. $P < 0.05$ was considered to be statistically significant.

RESULTS

AngII causes CMVEC dysfunction

First, purchased CMVECs were verified via microscopy. Cells were polygonal- or spindle-shaped and grew in a paving stone pattern (Figure 1A). Flow cytometry manifested that the molecular marker CD31 was positively expressed in these cells (Figure 1B), indicating that the purchased CMVECs were of high purity. Different concentrations of AngII were used to treat CMVECs and their effects were determined. Cell morphology observation indicated that CMVECs were morphologically damaged, with elongated or wrinkled shape, loss of arrangement regularity, and decreased cell number, after AngII treatment in a concentration-dependent manner (Figure 1C). MTT, scratch, tube formation, and flow cytometry assays exhibited that the proliferative, migratory, and angiogenic capacities were strikingly diminished, whereas the apoptotic capacity was remarkably augmented with increasing AngII concentrations in CMVECs (*$P < 0.05$; Figure 1D–G). Moroever, NO levels in CMVECs were appreciably reduced with increasing AngII concentrations (*$P < 0.05$; Figure 1H). Western blotting revealed that AngII considerably upregulated vWF and ET-1 levels and downregulated MnSOD and eNOS levels in CMVECs (*$P < 0.05$; Figure 1I). As 10^{-5} M AngII decreased CMVEC viability to 50% and caused obvious endothelial dysfunction, this concentration was selected to treat CMVECs in subsequent experiments.
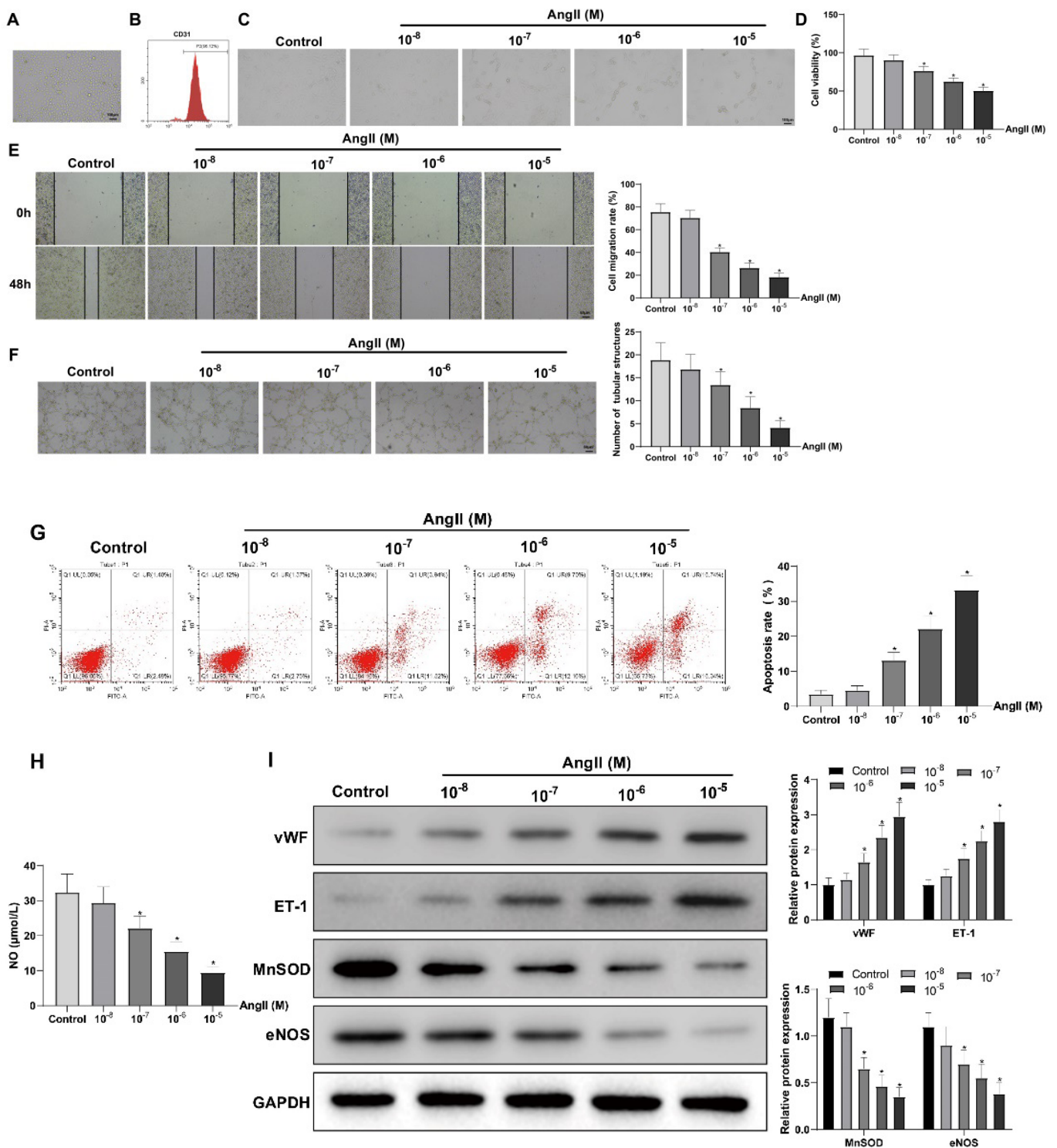
FIGURE 1 - AngII treatment leads to CMVEC dysfunction.

Notes: (A) The morphology of CMVECs was observed with a microscope (Olympus MK, Tokyo, Japan). (B) CD31 expression was measured by flow cytometry. CMVECs were treated with different concentrations of AngII. (C) The morphology of CMVECs was observed. (D) Cell viability was examined by MTT assay. (E) Cell migratory capacity was assessed by scratch assay. (F) Angiogenic capacity of CMVECs was evaluated by tubule formation assay. (G) Cell apoptotic capacity was determined by flow cytometry. (H) NO levels were tested with a kit. (I) vWF, ET-1, MnSOD, and eNOS protein expression was detected by western blot. Data were displayed as mean ± standard deviation, N = 3. *$P < 0.05$ compared with the control group. AngII, angiotensin II; CMVEC, cardiac microvascular endothelial cell; NO, nitric oxide; vWF, von Willebrand factor; ET-1, endothelin-1; MnSOD, manganese superoxide dismutase; eNOS, endothelial NO synthase.

EUE attenuates AngII-induced CMVEC dysfunction

To determine whether EUE attenuates AngII-induced CMVEC dysfunction, CMVECs were treated with different concentrations of EUE (0.25, 0.5, 1, and 2 mg/mL) and AngII. We found that EUE improved AngII-induced morphological damage in CMVECs (Figure 2A). Functional phenotype experiments revealed that EUE enhanced the cell migratory, proliferative, and angiogenic capacities and reduced the apoptotic capacity of AngII-induced CMVECs (*$P < 0.05$; Figure 2B–E). Additionally, EUE conspicuously augmented NO levels in AngII-induced CMVECs (*$P < 0.05$; Figure 2F). Western blot exhibited that EUE noticeably lowered vWF and ET-1 levels and increased MnSOD and eNOS levels in AngII-induced CMVECs (*$P < 0.05$; Figure 2G). Notably, no apparent improvement in CMVEC dysfunction was observed with EUE concentration > 1 mg/mL; therefore, 1 mg/mL EUE was selected to treat CMVECs in subsequent experiments. These results indicate that EUE attenuates AngII-induced CMVEC dysfunction.
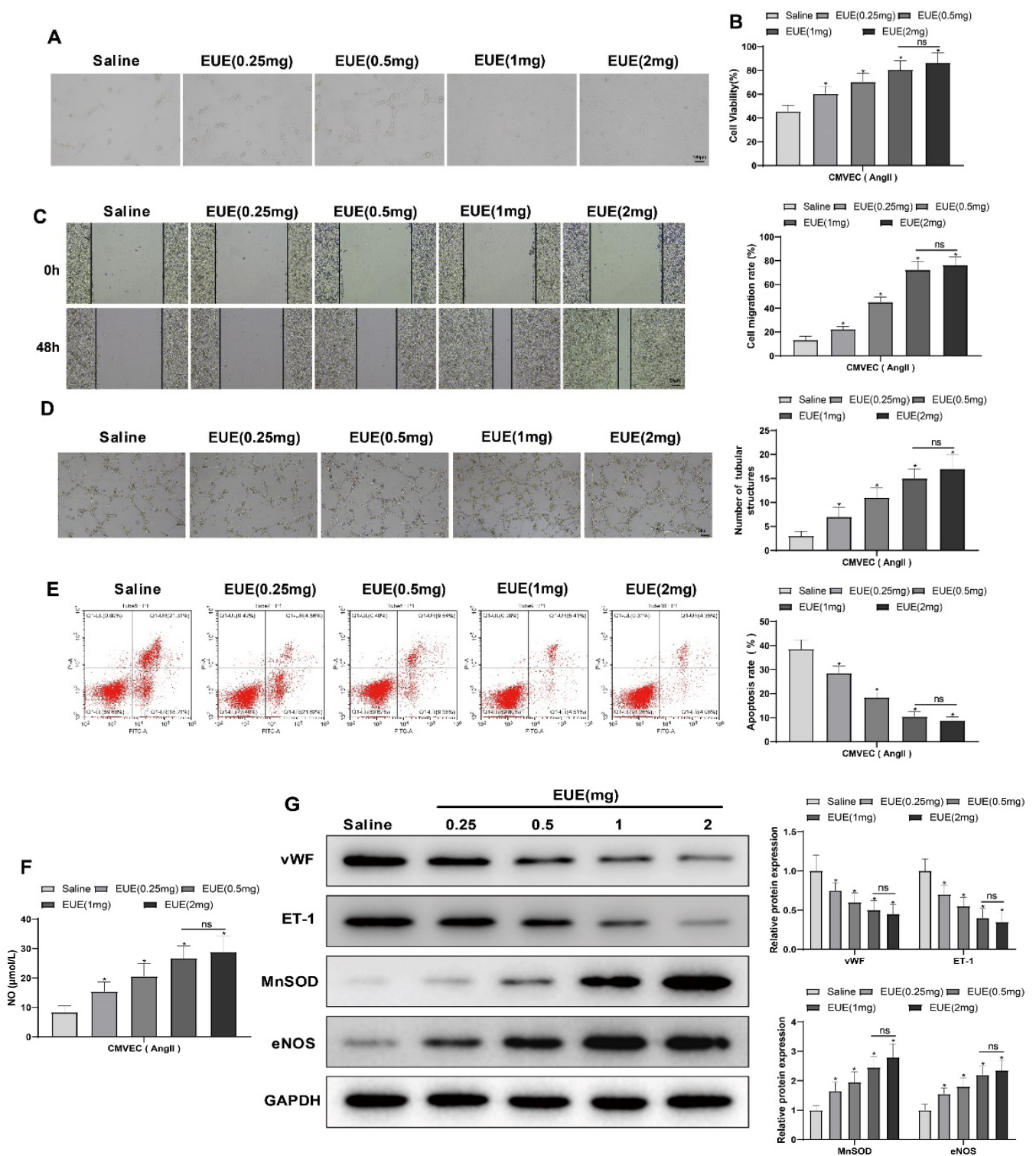
FIGURE 2 - AngII-induced CMVEC dysfunction is relieved by EUE.

Notes: CMVECs were treated with different concentrations of EUE and AngII. (A) The morphology of CMVECs was observed. (B) Cell viability was tested by MTT assay. (C) Cell migration was determined by scratch assay. (D) Angiogenic ability of cells was evaluated by tubule formation assay. (E) Apoptosis rate was measured by flow cytometry. (F) NO levels were assessed with a kit. (G) vWF, ET-1, MnSOD, and eNOS protein expression was examined by western blot. Data were displayed as mean ± standard deviation, N = 3. *$P < 0.05$ compared with the saline group. AngII, angiotensin II; CMVEC, cardiac microvascular endothelial cell; EUE, Eucommia ulmoides extract; NO, nitric oxide; vWF, von Willebrand factor; ET-1, endothelin-1; MnSOD, manganese superoxide dismutase; eNOS, endothelial NO synthase.

EUE restricts *p53* activation in AngII-induced CMVECs

RT-qPCR and western blot were used to determine *p53* expression. *p53* mRNA levels, accumulation of p-p53 in the nucleus, and p53 protein levels in the cytoplasm were dramatically elevated in CMVECs after AngII induction (*$P < 0.05$; Figure 3A–B). However, treatment with 1 mg/mL EUE reversed these effects (#$P < 0.05$; Figure 3C–D). These results indicate that EUE represses the activation of *p53* in dysfunctional CMVECs.
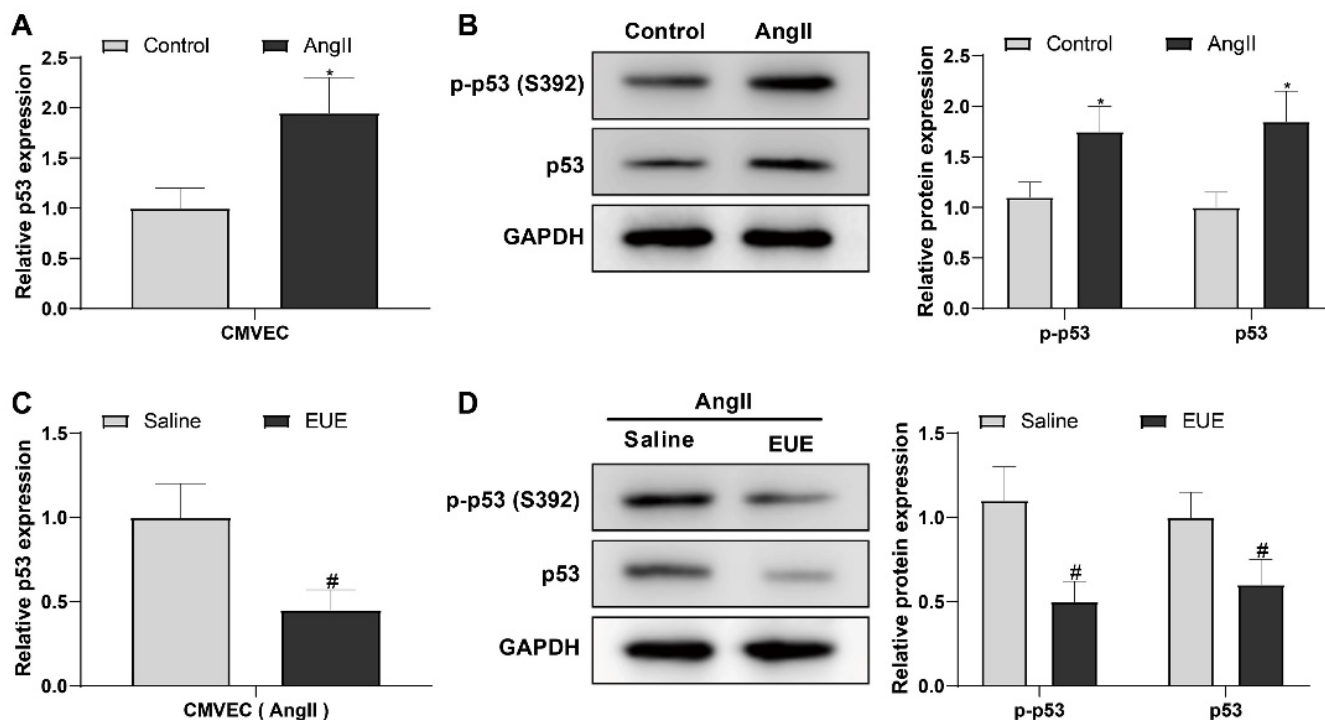
FIGURE 3 - EUE represses p53 activation in dysfunctional CMVECs.

Notes: CMVECs were treated with AngII. (A) p53 mRNA levels were determined by RT-qPCR. (B) p53 and p-p53 protein expression was examined by western blot. CMVECs were treated with 1 mg/mL EUE and AngII. (C) p53 mRNA levels were determined by RT-qPCR; (D) p53 and p-p53 protein expression was examined by western blot. Data were displayed as mean ± standard deviation, N = 3. *$P < 0.05$ compared with the control group; #$P < 0.05$ compared with the saline group. AngII, angiotensin II; CMVEC, cardiac microvascular endothelial cell; EUE, Eucommia ulmoides extract.

EUE attenuates AngII-induced CMVEC dysfunction by restraining *p53* activation

Next, to determine whether EUE attenuates AngII-induced CMVEC dysfunction by repressing *p53* activation, CMVECs were treated with EUE, p53 protein activator WR-1065 (100 µmol/L) (Rodkin *et al.*, 2020), and AngII. RT-qPCR and western blot revealed that WR-1065 enhanced *p53* mRNA levels, p-p53 accumulation in the nucleus, and p53 protein levels in the cytoplasm of AngII-induced CMVECs after EUE treatment (#$P < 0.05$; Figure 4A). WR-1065 further aggravated AngII-induced morphological damage in CMVECs after EUE treatment (Figure 4B). Compared with EUE treatment alone, co-treatment with EUE and WR-1065 apparently impeded the migratory, proliferative, and angiogenic capacities and facilitated the apoptosis of CMVECs (#$P < 0.05$; Figure 4C–F). Compared with EUE treatment alone, combined treatment with EUE and WR-1065 prominently reduced NO levels in AngII-induced CMVECs (#$P < 0.05$; Figure 4G). In contrast to EUE treatment alone, western blot revealed that co-treatment with EUE and WR-1065 noticeably restored vWF and ET-1 expression and reduced MnSOD and eNOS expression (#$P < 0.05$; Figure 4H). Therefore, EUE attenuates AngII-induced CMVEC dysfunction by restraining *p53* activation.
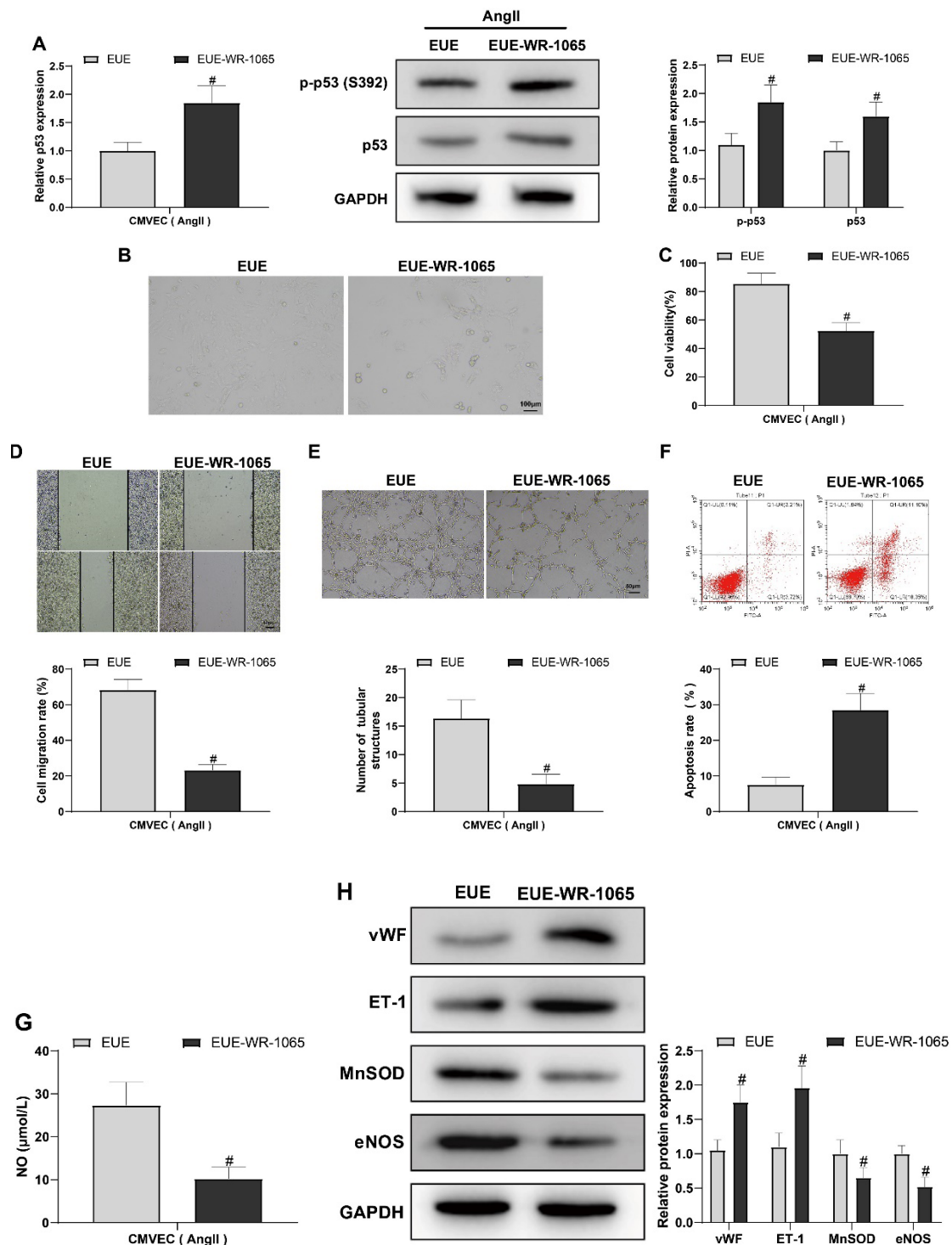
FIGURE 4 - EUE improves AngII-induced CMVEC dysfunction via p53 inactivation.

Notes: CMVECs were treated with EUE alone or with p53 protein activator WR-1065 before AngII induction. (A) p53 mRNA levels were examined by RT-qPCR and p53 and p-p53 protein expression was examined by western blot. (B) The morphology of CMVECs was observed. (C) Cell viability was evaluated by MTT assay. (D) Cell migration was tested by scratch assay. (E) Angiogenic ability of CMVECs was assessed by tubule formation assay. (F) Apoptosis of CMVECs was determined by TUNEL staining. (G) NO levels were measured with a kit. (H) vWF, ET-1, MnSOD, and eNOS protein expression was determined by western blot. Data were displayed as mean ± standard deviation, N = 3. #$P < 0.05$ compared with the EUE group. AngII, angiotensin II; CMVEC, cardiac microvascular endothelial cell; EUE, Eucommia ulmoides extract; NO, nitric oxide; vWF, von Willebrand factor; ET-1, endothelin-1; MnSOD, manganese superoxide dismutase; eNOS, endothelial NO synthase.

EUE attenuates AngII-induced CMVEC dysfunction by upregulating *HIF-1α* and *VEGF* levels via *p53* inactivation

To determine whether EUE affects *HIF-1α* and *VEGF* expression by inactivating *p53* to attenuate AngII-induced CMVEC dysfunction, we determined HIF-1α and VEGF expression before and after treatment with AngII, EUE, and WR-1065 using RT-qPCR and western blot. *HIF-1α* and *VEGF* levels were substantially reduced (*$P < 0.05$; Figure 5A–B) but restored by 1 mg/mL EUE treatment (*$P < 0.05$) in AngII-induced CMVECs, and this effect was counteracted by WR-1065 ([#]$P < 0.05$; Figure 5C–D). These findings indicate that EUE attenuates AngII-induced CMVEC dysfunction by elevating *HIF-1α* and *VEGF* expression via *p53* inactivation.
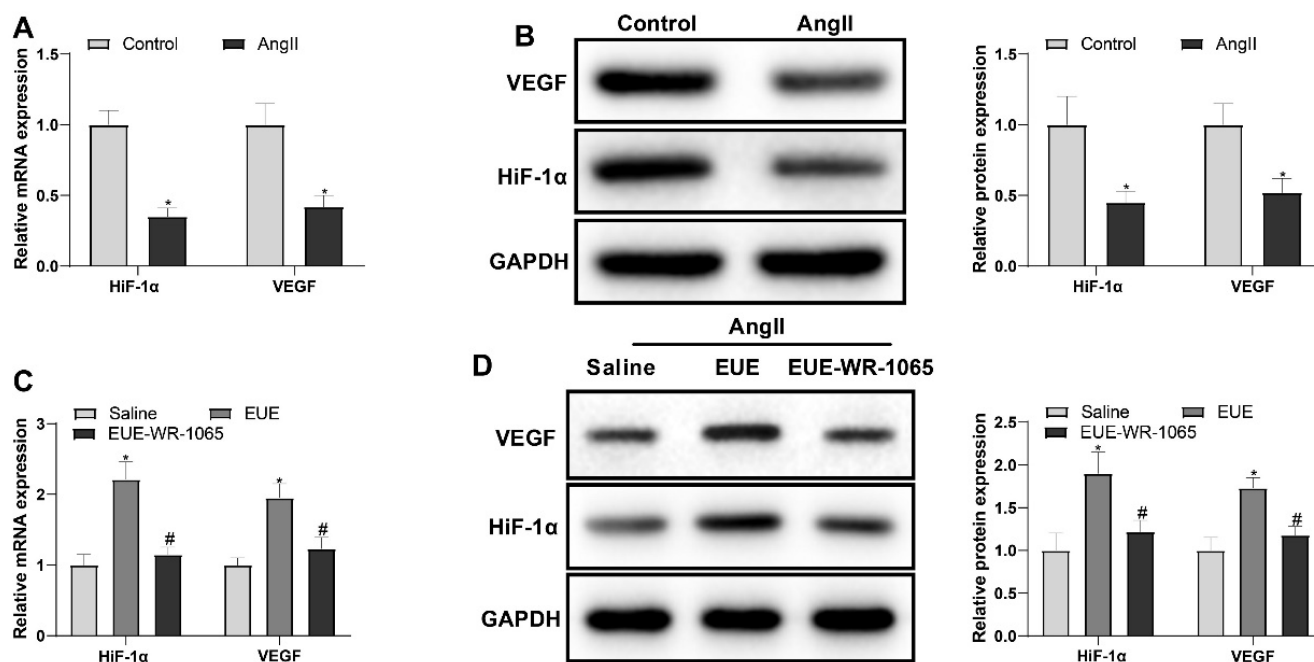
FIGURE 5 - EUE upregulates Hif-1α and VEGF expression by inactivating p53 to alleviate AngII-induced CMVEC dysfunction.

Note: (A) Hif-1α and VEGF expression was assessed by RT-qPCR in CMVECs. (B) Hif-1α and VEGF expression was assessed by western blot in CMVECs before and after AngII treatment. (C) Hif-1α and VEGF expression was assessed by RT-qPCR in AngII-induced CMVECs after treatment with normal saline, EUE, or EUE + WR-1065. (D) Hif-1α and VEGF expression was assessed by western blot in AngII-induced CMVECs after treatment with normal saline, EUE, or EUE + WR-1065. Data were displayed as mean ± standard deviation, N = 3. *$P < 0.05$ compared with the control or saline group; [#]$P < 0.05$ compared with the EUE group. AngII, angiotensin II; CMVEC, cardiac microvascular endothelial cell; EUE, Eucommia ulmoides extract; Hif-1α, hypoxia-inducible factor-1α; VEGF, vascular endothelial growth factor.

DISCUSSION

CMVECs regulate vessel tone via the release of diastolic and contractile factors derived from the endothelium and regulation and degradation of vasoactive peptides and enzymes on the surface of the endothelium in cardiomyocytes (Liu *et al.*, 2017). Endothelial function is crucial for maintaining vascular homeostasis. Endothelial dysfunction, primarily caused by the diminished action or production of relaxing mediators such as NO, is a marker of multiple cardiovascular conditions related to pathologies, such as vasoconstriction, inflammation, and thrombosis (Godo, Shimokawa, 2017). Therefore, CMVEC dysfunction should be explored further to understand the pathogenesis of cardiovascular diseases. Herein, EUE was found to attenuate AngII-induced

CMVEC dysfunction by elevating *HIF-1α* and *VEGF* expression via *p53* inactivation.

At rest, endothelial cells release vasodilators, such as NO. On activation, their signalling switches from the silencing of cell processes mediated by NO to redox signalling, which predisposes vessels to constriction by releasing thrombin, ET-1, AngII, and other molecules (Leite *et al.*, 2020). AngII overload induces endothelial cell injury, ultimately resulting in rarefaction of coronary microvessels and dysfunction of microvessels (Li *et al.*, 2021). AngII induces apoptosis in primary rat CMVECs in a dose-dependent manner (Wang *et al.*, 2019). Exosomal microRNA (miR)-29a induced by AngII attenuates the migratory, proliferative, and angiogenic capacities of CMVECs (Li *et al.*, 2022). In this study, the proliferative, migratory, and angiogenic capacities of CMVECs were prominently subdued, but their apoptotic rate was augmented with increasing AngII concentrations. NO levels in CMVECs were drastically reduced with increasing concentrations of AngII. eNOS is the enzyme responsible for NO production in the endothelium of blood vessels and is expressed in the endothelial cells of the heart (Chen *et al.*, 2020). vWF is a classical circulating hallmark of endothelial dysfunction (Leite *et al.*, 2020). MnSOD is a critical antioxidant mitochondrial enzyme, and its deficiency with age changes the responsiveness of endothelium-dependent vessels, which is a well-accepted standard for measuring endothelial function (Dang *et al.*, 2015; Glover *et al.*, 2014). Intriguingly, this study exhibited that AngII treatment remarkably enhanced the expression of endothelial function-related proteins, vWF and ET-1, and reduced the levels of MnSOD and eNOS, indicating that AngII contributes to CMVEC dysfunction.

EUE exerts anti-hypertensive, antioxidant, and anti-neoplastic effects, with an overall favourable security profile (Luo *et al.*, 2020). Aucubin, extracted from the seeds of *E. ulmoides*, exerts anti-apoptotic and anti-inflammatory effects and improves cardiac dysfunction, apoptosis, inflammation, and oxidative stress caused by lipopolysaccharides (Duan *et al.*, 2019). Different extracts of *E. ulmoides* and lignans can constrain hypertension by inhibiting inward calcium flow and cAMP activity,

modulating the renin–angiotensin system and NO levels, relaxing the blood vessels, and increasing the coronary flow (He *et al.*, 2014). *E. ulmoides* leaf extract recovers the function of the vascular endothelium and enhances NO levels in oxidised low-density lipoprotein-induced human umbilical vein endothelial cells, thereby protecting them against vascular disorders (Lee *et al.*, 2018). Moreover, *E. ulmoides* leaves increase eNOS and eNOS-produced NO levels to ameliorate renal haemodynamics and blood pressure (Ishimitsu *et al.*, 2021). In this study, we demonstrated that EUE elevated NO, MnSOD, and eNOS levels and proliferative, migratory, and angiogenic capacities and decreased apoptosis and vWF and ET-1 expression in AngII-induced CMVECs, indicating that EUE improves AngII-induced CMVEC dysfunction. Moreover, *E. ulmoides* affects the cardiac function via multiple pathways. For instance, pinoresinol diglucoside, an active compound of *E. ulmoides*, restrains cardiomyocyte inflammation and fibrosis via the protein kinase B/mammalian target of the rapamycin/nuclear factor kappa B pathway (Chen *et al.*, 2021). In addition, aucubin suppresses pressure overload-induced cardiac remodelling via β3-adrenoceptor-neuronal NOS cascades (Wu *et al.*, 2018). Lignan extracts from *E. ulmoides* Oliv. bark protect against hypertensive cardiac remodelling by depleting aldose reductase levels (Li *et al.*, 2013). Therefore, further studies are necessary to explore other pathways modulated by EUE in heart disease.

Overexpression of p53 drastically abrogates the anti-apoptotic ability of hypoxia-induced pulmonary CMVECs (Cao *et al.*, 2016). p53 functions can be affected by its decreased expression or activity in the nucleus (Nagpal, Yuan, 2021). AngII curbs the angiogenic ability of CMVECs and facilitates the accumulation and phosphorylation of cytosolic p53, thereby increasing p-p53 levels in the nucleus (Guan *et al.*, 2013). Upregulated p53 exerts anti-angiogenic effects and promotes programmed cell death and cell cycle arrest, and modulates metabolism, leading to the development of cardiovascular diseases (Men *et al.*, 2021). Interestingly, AngII treatment upregulated *p53* mRNA levels, nuclear p-p53 protein levels, and cytoplasmic p53 protein levels in CMVECs in this study, which were reversed by

EUE treatment, suggesting that EUE suppresses the activation of *p53* in dysfunctional CMVECs. Moreover, p53 activator abolished the repressive effects of EUE on AngII-induced CMVEC dysfunction.

HIF-1α activation contributes to Casitas B-cell lymphoma-induced exacerbation of AngII-induced cardiac hypertrophy (Yang *et al.*, 2021), suggesting a possible association between AngII and *HIF-1α*. VEGF, a growth factor with pro-angiogenic properties, exerts anti-apoptotic and mitogenic effects, facilitates cell migration, and enhances the vascular permeability of endothelial cells (Melincovici *et al.*, 2018). *HIF-1α* modulates *VEGF* transcriptional activation under hypoxic conditions (Zhang, Lv, Wang, 2018). In this study, we found that AngII reduced *HIF-1α* and *VEGF* expression in CMVECs, which was abrogated by EUE treatment. A previous study illustrated that p53 upregulation diminishes HIF-1α activity and expression and VEGF production in renal cell carcinoma cells (Lee *et al.*, 2020). Consistently, our data also revealed that the *p53* activator, WR-1065, reversed the upregulation of *HIF-1α* and *VEGF* levels by EUE in AngII-induced CMVECs. Consistent with our findings, a previous study proposed that overexpression of long non-coding RNA maternally expressed gene 3 mitigates AngII-induced damage in human umbilical vein endothelial cells by upregulating *HIF-1α* and *VEGF* levels and downregulating *p53* levels (Song *et al.*, 2019).

In conclusion, AngII induced CMVEC dysfunction, which was ameliorated by EUE by elevating *HIF-1α* and *VEGF* expression via *p53* inactivation. Our findings provide novel insights into the impact of EUE on CMVEC dysfunction and may be helpful to develop effective therapeutic strategies for cardiovascular diseases.

DECLARATION OF INTEREST

The authors declare that they have no competing interests.

FUNDING

REFERENCES

Cao P, Ma B, Sun D, Zhang W, Qiu J, Qin L, et al. Hsa_Circ_0003410 Promotes Hepatocellular Carcinoma Progression by Increasing the Ratio of M2/M1 Macrophages through the Mir-139-3p/Ccl5 Axis. Cancer Sci. 2022;113(2):634-47.

Cao Y, Jiang Z, Zeng Z, Liu Y, Gu Y, Ji Y, et al. Bcl-2 silencing attenuates hypoxia-induced apoptosis resistance in pulmonary microvascular endothelial cells. Apoptosis. 2016;21(1):69-84.

Chen G, Xu C, Gillette TG, Huang T, Huang P, Li Q, et al. Cardiomyocyte-derived small extracellular vesicles can signal enos activation in cardiac microvascular endothelial cells to protect against ischemia/reperfusion injury. Theranostics. 2020;10(25):11754-74.

Chen Y, Pan R, Zhang J, Liang T, Guo J, Sun T, et al. Pinoresinol diglucoside (PDG) attenuates cardiac hypertrophy Via AKT/mTOR/NF-Kappab signaling in pressure overload-induced rats. J Ethnopharmacol. 2021;272:113920.

Dang Y, Ling S, Duan J, Ma J, Ni R, Xu JW. Bavachalcone-induced manganese superoxide dismutase expression through the amp-activated protein kinase pathway in human endothelial cells. Pharmacology. 2015;95(3-4):105-10.

Duan M, Yuan Y, Liu C, Cai Z, Xie Q, Hu T, et al. Indigo fruits ingredient, aucubin, protects against LPS-induced cardiac dysfunction in mice. J Pharmacol Exp Ther. 2019;371(2):348-59.

Ames MK, Atkins CE, Pitt B. Erratum for the Renin-angiotensin-aldosterone system and its suppression. J Vet Intern Med. 2019;33(5):2551.

Fan L, Zhou W, Zhang L, Jiang D, Zhao Q, Liu L. Sitagliptin protects against Hypoxia/Reoxygenation (H/R)-induced cardiac microvascular endothelial cell injury. Am J Transl Res. 2019;11(4):2099-107.

Glover M, Hebert VY, Nichols K, Xue SY, Thibeaux TM, Zavecz JA, et al. Overexpression of mitochondrial antioxidant Manganese Superoxide Dismutase (Mnsod) provides protection against Azt- or 3tc-induced endothelial dysfunction. Antiviral Res. 2014;111:136-42.

Godo S, Shimokawa H. Endothelial functions. Arterioscler Thromb Vasc Biol. 2017;37(9):e108-e14.

Guan A, Gong H, Ye Y, Jia J, Zhang G, Li B, et al. Regulation of P53 by Jagged1 Contributes to Angiotensin Ii-Induced Impairment of Myocardial Angiogenesis. PLoS One. 2013;8(10):e76529.

He X, Wang J, Li M, Hao D, Yang Y, Zhang C, et al. Eucommia ulmoides oliv.: Ethnopharmacology, phytochemistry and

pharmacology of an important Traditional Chinese Medicine. J Ethnopharmacol. 2014;151(1):78-92.

Ishimitsu A, Tojo A, Satonaka H, Ishimitsu T. Eucommia ulmoides (Tochu) and its extract geniposidic acid reduced blood pressure and improved renal hemodynamics. Biomed Pharmacother. 2021;141:111901.

Kim DY, Piao J, Hong HS. Substance-P inhibits cardiac microvascular endothelial dysfunction caused by high glucose-induced oxidative stress. Antioxidants (Basel). 2021;10(7):1084.

Lee GH, Lee HY, Choi MK, Choi AH, Shin TS, Chae HJ. Eucommia ulmoides leaf (EUL) extract enhances no production in ox-LDL-treated human endothelial cells. Biomed Pharmacother. 2018;97:1164-72.

Lee MK, Kim MJ, Cho SY, Park SA, Park KK, Jung UJ, et al. Hypoglycemic effect of Du-Zhong (Eucommia Ulmoides Oliv.) leaves in streptozotocin-induced diabetic rats. Diabetes Res Clin Pract. 2005;67(1):22-8.

Lee SH, Kang JH, Ha JS, Lee JS, Oh SJ, Choi HJ, et al. Transglutaminase 2-mediated p53 depletion promotes angiogenesis by increasing HIF-1alpha-p300 binding in renal cell carcinoma. Int J Mol Sci. 2020;21(14):5042.

Leite AR, Borges-Canha M, Cardoso R, Neves JS, Castro-Ferreira R, Leite-Moreira A. Novel biomarkers for evaluation of endothelial dysfunction. Angiology. 2020;71(5):397-410.

Li DX, Chen W, Jiang YL, Ni JQ, Lu L. Antioxidant protein peroxiredoxin 6 suppresses the vascular inflammation, oxidative stress and endothelial dysfunction in angiotensin II-induced endotheliocyte. Gen Physiol Biophys. 2020;39(6):545-55.

Li F, Wang J, Song Y, Shen D, Zhao Y, Li C, et al. Qiliqiangxin alleviates Ang II-Induced CMECS apoptosis by downregulating autophagy via the ErbB2-AKT-FoxO3a axis. Life Sci. 2021;273:119239.

Li G, Qiu Z, Li C, Zhao R, Zhang Y, Shen C, et al. Exosomal MiR-29a in cardiomyocytes induced by angiotensin II regulates cardiac microvascular endothelial cell proliferation, migration and angiogenesis by targeting VEGFA. Curr Gene Ther. 2022;

Li LM, Zheng B, Zhang RN, Jin LS, Zheng CY, Wang C, et al. Chinese medicine Tongxinluo increases tight junction protein levels by inducing KLF5 expression in microvascular endothelial cells. Cell Biochem Funct. 2015;33(4):226-34.

Li X, Gui Z, Liu H, Qian S, Jia Y, Luo X. Remifentanil pretreatment ameliorates H/R-induced cardiac microvascular endothelial cell dysfunction by regulating the Pi3k/Akt/Hif-1alpha signaling pathway. Bioengineered. 2021;12(1):7872-81.

Li ZY, Gu J, Yan J, Wang JJ, Huang WH, Tan ZR, et al. Hypertensive cardiac remodeling effects of lignan extracts from eucommia ulmoides oliv. Bark--a famous traditional Chinese medicine. Am J Chin Med. 2013;41(4):801-15.

Liao Z, Chen Y, Duan C, Zhu K, Huang R, Zhao H, et al. Cardiac telocytes inhibit cardiac microvascular endothelial cell apoptosis through exosomal mirna-21-5p-targeted CDIP1 silencing to improve angiogenesis following myocardial infarction. Theranostics. 2021;11(1):268-91.

Liu B, Li CP, Wang WQ, Song SG, Liu XM. Lignans extracted from eucommia ulmoides oliv. protects against ages-induced retinal endothelial cell injury. Cell Physiol Biochem. 2016;39(5):2044-54.

Liu C, Guo FF, Xiao JP, Wei JY, Tang LY, Yang HJ. [Research Advances in Chemical Constituents and Pharmacological Activities of Different Parts of Eucommia Ulmoides]. Zhongguo Zhong Yao Za Zhi. 2020;45(3):497-512.

Liu E, Han L, Wang J, He W, Shang H, Gao X, et al. eucommia ulmoides bark protects against renal injury in cadmium-challenged rats. J Med Food. 2012;15(3):307-14.

Liu Y, Zou J, Li B, Wang Y, Wang D, Hao Y, et al. Runx3 modulates hypoxia-induced endothelial-to-mesenchymal transition of human cardiac microvascular endothelial Cells. Int J Mol Med. 2017;40(1):65-74.

Long L, Zhang X, Wen Y, Li J, Wei L, Cheng Y, et al. Qingda granule attenuates angiotensin II-induced renal apoptosis and activation of the P53 pathway. Front Pharmacol. 2021;12:770863.

Luo LF, Wu WH, Zhou YJ, Yan J, Yang GP, Ouyang DS. Antihypertensive effect of eucommia ulmoides oliv. extracts in spontaneously hypertensive rats. J Ethnopharmacol. 2010;129(2):238-43.

Luo X, Wu J, Li Z, Jin W, Zhang F, Sun H, et al. Safety Evaluation of Eucommia Ulmoides Extract. Regul Toxicol Pharmacol. 2020;118:104811.

Melincovici CS, Bosca AB, Susman S, Marginean M, Mihu C, Istrate M, et al. Vascular Endothelial Growth Factor (Vegf) - Key factor in normal and pathological angiogenesis. Rom J Morphol Embryol. 2018;59(2):455-67.

Men H, Cai H, Cheng Q, Zhou W, Wang X, Huang S, et al. the regulatory roles of p53 in cardiovascular health and disease. Cell Mol Life Sci. 2021;78(5):2001-18.

Nagpal I, Yuan ZM. The Basally Expressed P53-Mediated Homeostatic Function. Front Cell Dev Biol. 2021;9(775312.

Naryzhny SN, Legina OK. Structural-Functional Diversity of P53 Proteoforms. Biomed Khim. 2019;65(4):263-76.

Eucommia ulmoides extract attenuates angiotensin II-induced cardiac microvascular endothelial cell dysfunction by inactivating *p53*

Park SA, Choi MS, Jung UJ, Kim MJ, Kim DJ, Park HM, et al. Eucommia ulmoides oliver leaf extract increases endogenous antioxidant activity in type 2 Diabetic mice. J Med Food. 2006;9(4):474-9.

Qi J, Wang F, Yang P, Wang X, Xu R, Chen J, et al. Mitochondrial Fission Is Required for Angiotensin Ii-Induced Cardiomyocyte Apoptosis Mediated by a Sirt1-P53 Signaling Pathway. Front Pharmacol. 2018;9:176.

Rana NK, Singh P, Koch B. Cocl2 simulated hypoxia induce cell proliferation and alter the expression pattern of hypoxia associated genes involved in angiogenesis and apoptosis. Biol Res. 2019;52(1):12.

Rodkin S, Khaitin A, Pitinova M, Dzreyan V, Guzenko V, Rudkovskii M, et al. The localization of P53 in the crayfish mechanoreceptor neurons and its role in axotomy-induced death of satellite glial cells remote from the axon transection site. J Mol Neurosci. 2020;70(4):532-41.

Si R, Zhang Q, Tsuji-Hosokawa A, Watanabe M, Willson C, Lai N, et al. overexpression of p53 due to excess protein o-glcnacylation is associated with coronary microvascular disease in Type 2 diabetes. Cardiovasc Res. 2020;116(6):1186-98.

Song J, Huang S, Wang K, Li W, Pao L, Chen F, et al. Long Non-Coding Rna Meg3 Attenuates the Angiotensin Ii-Induced Injury of Human Umbilical Vein Endothelial Cells by Interacting with P53. Front Genet. 2019;10:78.

Wang JY, Yuan Y, Chen XJ, Fu SG, Zhang L, Hong YL, et al. Extract from eucommia ulmoides oliv. ameliorates arthritis via regulation of inflammation, synoviocyte proliferation and osteoclastogenesis in vitro and in vivo. J Ethnopharmacol. 2016;194:609-16.

Wang Y, Fan Y, Song Y, Han X, Fu M, Wang J, et al. Angiotensin II induces apoptosis of cardiac microvascular endothelial cells via regulating Ptp1b/Pi3k/Akt pathway. In Vitro Cell Dev Biol Anim. 2019;55(10):801-11.

Wu QQ, Xiao Y, Duan MX, Yuan Y, Jiang XH, Yang Z, et al. Aucubin protects against pressure overload-induced cardiac remodelling via the Beta3 -Adrenoceptor-Neuronal Nos cascades. Br J Pharmacol. 2018;175(9):1548-66.

Yang Y, Zou P, He L, Shao J, Tang Y, Li J. CBL Aggravates Ang II-induced cardiac hypertrophy via the VHL/HIF-1alpha pathway. Exp Cell Res. 2021;405(2):112730.

Zeng ZM, Du HY, Xiong L, Zeng XL, Zhang P, Cai J, et al. Brca1 protects cardiac microvascular endothelial cells against irradiation by regulating P21-mediated cell cycle arrest. Life Sci. 2020;244:117342.

Zhang D, Lv FL, Wang GH. Effects of HIF-1alpha on diabetic retinopathy angiogenesis and VEGF expression. Eur Rev Med Pharmacol Sci. 2018;22(16):5071-76.

Zhang X, Qi Z, Yin H, Yang G. Interaction between p53 and Ras signaling controls cisplatin resistance via HDAC4- and HIF-1alpha-mediated regulation of apoptosis and autophagy. Theranostics. 2019;9(4):1096-114.